

Part 1

Introduction

1.1

Cellular Solids – Scaling of Properties

Michael F. Ashby

1.1.1

Introduction

Cellular solids – ceramics, polymers, metals – have properties that depend on both topology and material. Of the three classes, polymer foams are the most widely investigated, and it is from these studies that much of the current understanding derives. Recent advances in techniques for foaming metals has led to their intense study, extending the understanding. Of the three classes, ceramic foams are the least well characterized. Their rapidly growing importance as filters, catalyst supports, membranes, and scaffolds for cell growth has stimulated much recent work, making this book both relevant and timely.

The underlying principles that influence cellular properties are common to all three classes. Three factors dominate (Fig. 1):

- The properties of the solid of which the foam is made.
- The topology (connectivity) and shape of the cells.
- The relative density $\tilde{\rho}/\rho_s$ of the foam, where $\tilde{\rho}$ is the density of the foam and ρ_s that of the solid of which it is made.

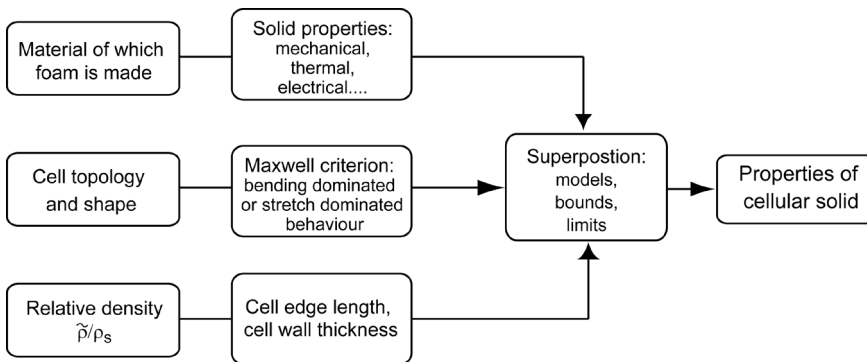


Fig. 1 Design variables. The properties of cellular materials depend on the material of the cell walls, the cell topology, and the relative density $\tilde{\rho}/\rho_s$. The contents of the boxes are explained in the text.

This chapter summarizes these principles, providing an introduction to the more specialized chapters that follow.

1.1.2

Cellular or “Lattice” Materials

A *lattice* is a connected network of struts. In the language of structural engineering, a lattice truss or space frame means an array of struts, pin-jointed or rigidly bonded at their connections, usually made of one of the conventional materials of construction: wood, steel, or aluminum. Their purpose is to create stiff, strong, load-bearing structures using as little material as possible, or, where this is useful, to be as light as possible. The word “lattice” is used in other contexts: in the language of crystallography, for example, a lattice is a hypothetical grid of connected lines with three-dimensional translational symmetry. The intersections of the lines define the atom sites in the crystal; the unit cell and symmetry elements of the lattice characterize the crystal class.

Here we are concerned with lattice or *cellular materials*. Like the trusses and frames of the engineer, these are made up of a connected array of struts or plates, and like the crystal lattice, they are characterized by a typical cell with certain symmetry elements; some, but not all, have translational symmetry. But lattice materials differ from the lattices of the engineer in one important regard: that of scale. That of the unit cell of lattice materials is one of millimeters or micrometers, and it is this that allows them to be viewed both as structures and as materials. At one level, they can be analyzed by using classical methods of mechanics, just as any space frame is analyzed. But at another we must think of the lattice not only as a set of connected struts, but as a “material” in its own right, with its own set of effective properties, allowing direct comparison with those of monolithic materials.

Historically, *foams*, a particular subset of lattice-structured materials, were studied long before attention focused on lattices of other types. Early studies assumed that foam properties depended linearly on relative density $\tilde{\rho}/\rho_s$ (i.e., the volume fraction of solid in the material), but for most foams this is not so. A sound understanding of their mechanical properties began to emerge in the 1960s and 1970 with the work of Gent and Thomas [1] and Patel and Finnie [2]. Work since then has built a comprehensive understanding of mechanical, thermal, and electrical properties of foams, summarized in the texts “Cellular Solids” [3], “Metal Foams, a Design Guide” [4], and a number of conference proceedings [5–9]. The ideas have been applied with success to ceramic foams, notably by Green et al. [10–13], Gibson et al. [14–17], and Vedula et al. [18, 19].

The central findings of this body of research are summarized briefly in Section 1.1.3. One key finding is that the deformation of most foams, whether open- or closed-cell, is *bending-dominated* – a term that is explained more fully below. A consequence of this is that their stiffnesses and strength (at a given relative density) fall far below the levels that would be expected of *stretch-dominated* structures, typified by a fully triangulated lattice. To give an idea of the difference: a low-connectivity

lattice, typified by a foam, with a relative density of 0.1 (meaning that the solid cell walls occupy 10% of the volume) is less stiff by a factor of 10 than a stretch-dominated, triangulated lattice of the same relative density.

In this section we explore the significant features of both bending- and stretch-dominated structures, using dimensional methods to arrive at simple, approximate scaling laws for mechanical, thermal, and electrical properties. Later chapters deal with these in more detail; the merit of the method used here is that of retaining physical clarity and mathematical simplicity. The aim is to provide an overview, setting the scene for what is to come.

1.1.3

Bending-Dominated Structures

Figure 2 is an image of an open-cell foam. It typifies one class of lattice-structured material. It is made up of struts connected at joints, and the characteristic of this class is the low connectivity of the joints (the number of struts that meet there).

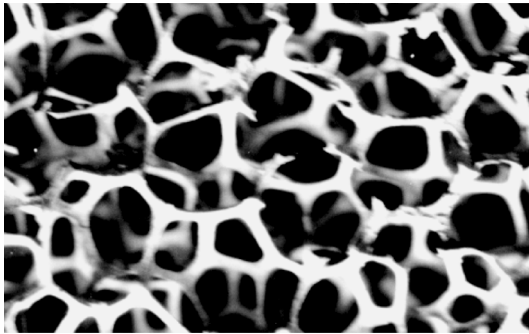


Fig. 2 A typical cellular structure. The topology of the cells causes the cell edges to bend when the structure is loaded. Even when the cells are closed, the deformation is predominantly bending because the thin cell faces buckle easily.

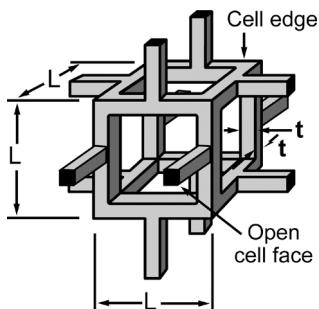


Fig. 3 An idealized cell in an open-cell foam.

Figure 3 is an idealization of a unit cell of the structure. It consists of solid struts surrounding a void space containing a gas or fluid. Lattice-structured materials (often called cellular solids) are characterized by their relative density, which for the structure shown here (with $t \ll L$) is

$$\frac{\tilde{\rho}}{\rho_s} \propto \left(\frac{t}{L}\right)^2 \tag{1}$$

where $\tilde{\rho}$ is the density of the foam, ρ_s is the density of the solid of which it is made, L is the cell size, and t is the thickness of the cell edges.

1.1.3.1

Mechanical Properties

Figure 4 shows the compressive stress–strain curve of bending-dominated lattice. The material is linear-elastic, with modulus \tilde{E} up to its elastic limit, at which point the cell edges yield, buckle, or fracture. The structure continues to collapse at a

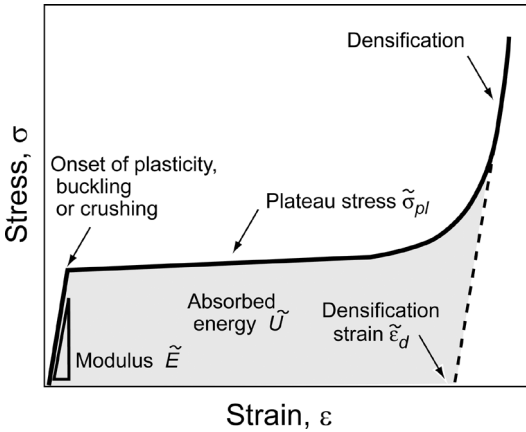


Fig. 4 Stress–strain curve of a cellular solid, showing the important parameters.

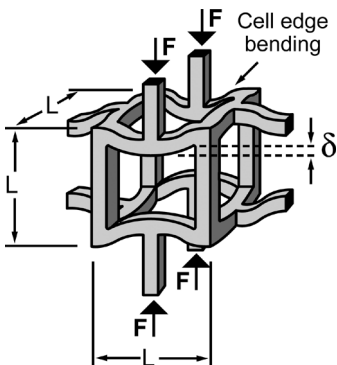


Fig. 5 When a low-connectivity structure is loaded, the cell edges bend, giving a low modulus.

nearly constant stress (plateau stress $\tilde{\sigma}_{pl}$) until opposite sides of the cells impinge (densification strain $\tilde{\epsilon}_d$), when the stress rises steeply. The three possible collapse mechanisms compete; the one that requires the lowest stress wins. The mechanical properties are calculated in the ways developed below, details of which can be found in Ref. [3].

A remote compressive stress σ exerts a force $F \propto \sigma L^2$ on the cell edges, causing them to bend, as shown in Fig. 5, with bending deflection δ . A strut of length L , loaded at its midpoint by a force F , deflects by a distance δ

$$\delta \propto \frac{FL^3}{E_s I} \quad (2)$$

where E_s is the modulus of the solid of which the strut is made, and $I = t^4/12$ the second moment of area of the cell edge of square cross section $t \times t$. The compressive strain suffered by the cell as a whole is then $\epsilon \propto 2\delta/L$. Assembling these results gives the modulus $\tilde{E} = \sigma/\epsilon$ of the foam as

$$\frac{\tilde{E}}{E_s} \propto \left(\frac{\tilde{\rho}}{\rho_s}\right)^2 \quad (\text{bending-dominated behavior}). \quad (3)$$

Since $\tilde{E} = E_s$ when $\tilde{\rho} = \rho_s$, we expect the constant of proportionality to be close to unity – a speculation confirmed both by experiment and by numerical simulation.

A similar approach can be used to model the collapse load, and thus the plateau stress of the structure. The cell walls yield, as shown in Fig. 6, when the force exerted on them exceeds their fully plastic moment

$$M_f = \frac{\sigma_{y,s} t^3}{4} \quad (4)$$

where $\sigma_{y,s}$ is the yield strength of the solid of which the foam is made. This moment is related to the remote stress by $M \propto FL \propto \sigma L^3$. Assembling these results gives the failure strength $\tilde{\sigma}_{pl}$:

$$\frac{\tilde{\sigma}_{pl}}{\sigma_{y,s}} \propto \left(\frac{\tilde{\rho}}{\rho_s}\right)^{3/2} \quad (\text{bending-dominated behavior}). \quad (5)$$

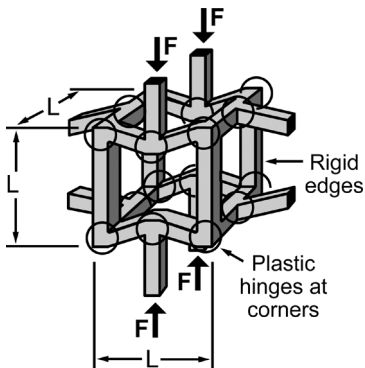


Fig. 6 Foams made of ductile materials collapse by plastic bending of the cell edges.

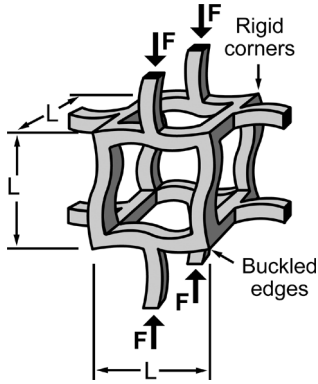


Fig. 7 An elastomeric foam collapses by elastic buckling of the cell edges.

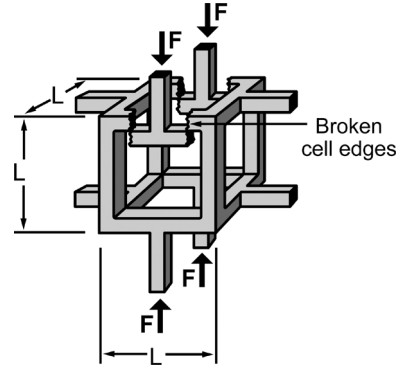


Fig. 8 A brittle foam collapses by successive fracturing of the cell edges. Ceramic foams generally show this collapse mechanism.

The constant of proportionality has been established both by experiment and by numerical computation; its value is approximately 0.3.

Elastomeric foams collapse not by yielding but by elastic buckling, and brittle foams by cell-wall fracture (Figs. 7 and 8). As with plastic collapse, simple scaling laws describe this behavior well. A strut of length L buckles under a compressive load F_b , the Euler buckling load, where

$$F_b \propto \frac{E_s I}{L^2} \propto \frac{E_s t^4}{L^2}. \quad (6)$$

Since $F = \sigma F^2$, the stress that causes the foam to collapse by elastic buckling $\tilde{\sigma}_{el}$ scales as

$$\frac{\tilde{\sigma}_{el}}{E_s} \propto \left(\frac{\tilde{\rho}}{\rho_s} \right)^2 \quad (\text{buckling-dominated behavior}). \quad (7)$$

More sophisticated modeling gives the constant of proportionality as 0.05. Cell walls fracture when the bending moment exceeds that given by Eq. (4) with $\sigma_{y,s}$ replaced by $\sigma_{cr,s}$, the modulus of rupture of a strut. The crushing stress therefore scales in the same way as the plastic collapse stress, giving

$$\frac{\tilde{\sigma}_{cr}}{\sigma_{cr,s}} \propto \left(\frac{\tilde{\rho}}{\rho_s} \right)^{3/2} \quad (\text{fracturing-dominated behavior}) \quad (8)$$

with a constant of proportionality of about 0.2.

Densification when the stress rises steeply is a purely geometric effect: the opposite sides of the cells are forced into contact and further bending or buckling is not possible. If we think of compression as a strain-induced increase in relative density, then simple geometry gives the densification strain $\tilde{\epsilon}_d$ as

$$\tilde{\epsilon}_d = 1 - \left(\frac{\tilde{\rho}}{\rho_s} \right) / \left(\frac{\rho_{crit}}{\rho_s} \right) \quad (9)$$

where $\rho_{\text{crit}}/\rho_s$ is the relative density at which the structure locks up. Experiments broadly support this estimate, and indicate a value for the lock up density as $\rho_{\text{crit}}/\rho_s \approx 0.6$.

Foamlike lattices are often used for cushioning, packaging, or to protect against impact, by utilizing the long, flat plateau of their stress–strain curves. The useful energy that they can absorb per unit volume \tilde{U} (Fig. 4) is approximated by

$$\tilde{U} \approx \tilde{\sigma}_{\text{pl}} \tilde{\epsilon}_d \quad (10)$$

where $\tilde{\sigma}_{\text{pl}}$ is the plateau stress – the yield, buckling, or fracturing strength of Equations (6), (7), or (8), whichever is least.

This bending-dominated behavior is not limited to open-cell foams with structures like that of Fig. 2. Most closed-cell foams also follow these scaling laws, at first sight an unexpected result because the cell faces must carry membrane stresses when the foam is loaded, and these should lead to a linear dependence of both stiffness and strength on relative density. The explanation lies in the fact that the cell faces are very thin; they buckle or rupture at stresses so low that their contribution to stiffness and strength is small, and the cell edges carry most of the load.

1.1.3.2

Thermal Properties

Cellular solids have useful heat-transfer properties. The cells are sufficiently small that convection of the gas within them is usually suppressed. Heat transfer through the lattice is then the sum of that conducted through the struts and that through the still air (or other fluid) contained in the cells. On average one-third of the struts lie parallel to each axis, and this suggests that the conductivity might be described by

$$\tilde{\lambda} = \frac{1}{3} \left(\frac{\tilde{\rho}}{\rho_s} \right) \lambda_s + \left(1 - \left(\frac{\tilde{\rho}}{\rho_s} \right) \right) \lambda_g. \quad (11)$$

Here the first term on the right describes conduction through the solid cell walls and edges (conductivity λ_s) and the second that through the gas contained in the cells (conductivity λ_g ; for dry air $\lambda_g = 0.025 \text{ W m}^{-1} \text{ K}^{-1}$). This is an adequate approximation for very low density foams, but it obviously breaks down as $\tilde{\rho}/\rho_s$ approaches unity. This is because joints are shared by the struts, and as $\tilde{\rho}/\rho_s$ rises, the joints occupy a larger and larger fraction of the volume. This volume scales as t^3/L^3 or, via Eq. (1), as $(\tilde{\rho}/\rho_s)^{3/2}$, so we need an additional term to allow for this:

$$\tilde{\lambda} = \frac{1}{3} \left(\left(\frac{\tilde{\rho}}{\rho_s} \right) + 2 \left(\frac{\tilde{\rho}}{\rho_s} \right)^{3/2} \right) \lambda_s + \left(1 - \left(\frac{\tilde{\rho}}{\rho_s} \right) \right) \lambda_g \quad (12)$$

which now correctly reduces to $\tilde{\lambda} = \lambda_s$ at $\tilde{\rho} = \rho_s$. The term associated with the gas, often negligible, becomes important in foams intended for thermal insulation, since these have a low relative density and a conductivity approaching λ_g .

The thermal diffusivities of lattice structures scale in a different way. Thermal diffusivity is defined as

$$a = \frac{\lambda}{\rho C_p} \quad (13)$$

where C_p is the specific heat in $\text{J kg}^{-1} \text{K}^{-1}$. The specific heat \tilde{C}_p of a cellular structure is the same as that of the solid of which it is made (because of its units). Thus, neglecting for simplicity any conductivity through the gas, we find the thermal diffusivity \tilde{a} to be

$$\tilde{a} = \frac{\tilde{\lambda}}{\tilde{\rho} \tilde{C}_p} \approx \frac{1}{3} \left(1 + 2 \left(\frac{\tilde{\rho}}{\rho_s} \right)^{1/2} \right) \frac{\lambda_s}{\rho_s C_{p,s}}. \quad (14)$$

a surprising result, since it is almost independent of relative density.

The thermal expansion coefficient of a cellular material is less interesting: it is the same as that of the solid from which it is made.

1.1.3.3

Electrical Properties

Insulating lattices are attractive as structural materials with low dielectric constant, which falls towards 1 (the value for air or vacuum) as the relative density decreases:

$$\tilde{\epsilon} = 1 + (\epsilon_s - 1) \left(\frac{\tilde{\rho}}{\rho_s} \right) \quad (15)$$

where ϵ_s is the dielectric constant of the solid of which the cell walls are made. Those that conduct have electrical conductivities that follow the same scaling law as the thermal conductivity (Eq. (11) with thermal conductivities replaced by electrical conductivities); here the conductivity of the gas can usually be ignored.

1.1.4

Maxwell's Stability Criterion

If lattice-structure materials with low strut connectivity, like those of Figs. 2 and 3, have low stiffness because the configuration of their cell edges allows them to bend, might it not be possible to devise other configurations in which the cell edges are made to stretch instead? This thinking leads to the idea of *microtruss lattice structures*. To understand these we need Maxwell's stability criterion, a deceptively simple yet profoundly fundamental rule [20].

The condition for a pin-jointed frame (i.e., one that is hinged at its joints) made up of b struts and j frictionless joints, like those in Fig. 9, to be both statically and kinematically determinate (i.e., it is rigid and does not fold up when loaded) in two dimensions, is:

$$M = b - 2j + 3 = 0. \quad (16)$$

In three dimensions the equivalent equation is

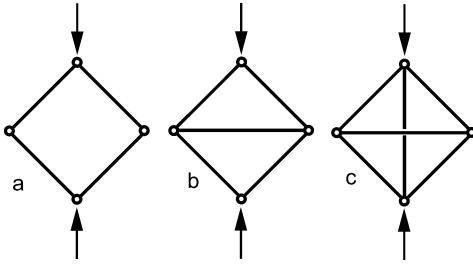


Fig. 9 The pin-jointed frame in a) folds up when loaded – it is a mechanism. If its joints are welded together the struts bend (as in Fig. 5) – it becomes a *bending-dominated structure*. The triangulated frame in b) is stiff when loaded because the transverse strut carries

tension – it is a *stretch-dominated structure*. The frame in c) is over-constrained; if the horizontal bar is shortened, the vertical one is put into tension even when no external loads are applied (giving a state of self-stress).

$$M = b - 3j + 6 = 0. \quad (17)$$

If $M < 0$, as in Fig. 9a, the frame is a *mechanism*; it has one or more degrees of freedom, and – in the directions that these allow displacements – it has no stiffness or strength. If its joints are locked (as they are in the lattice structures that concern us here) the bars of the frame *bend* when the structure is loaded, as in Fig. 5. If, instead, $M = 0$, as in Fig. 9b, the frame ceases to be a mechanism. If it is loaded, its members carry tension or compression (even when pin-jointed), and it becomes a *stretch-dominated* structure. Locking the joints now makes little difference because slender structures are much stiffer when stretched than when bent. There is an underlying principle here: the structural efficiency of stretch-dominated structures is high; that of bending-dominated structures is low.

Fig. 9c introduces a further concept, that of self-stress. It is a structure with $M > 0$. If the vertical strut is shortened, it pulls the other struts into compression, which is balanced by the tension it carries. The struts carry stress even though there are no external loads on the structure. The criteria of Eqs. (14) and (15) are necessary conditions for rigidity, but are not in general sufficient conditions, as they do not account for the possibility of states of self-stress and mechanisms. A generalization of the Maxwell rule in three dimensions is given by Calladine [21]:

$$M = b - 3j + 6 = s - m \quad (18)$$

where s and m are the number of states of self-stress and of mechanisms, respectively. Each can be determined by finding the rank of the equilibrium matrix that describes the frame in a full structural analysis [22]. A *just-rigid* framework (a lattice that is both statically and kinematically determinate) has $s = m = 0$. The nature of Maxwell's rule as a necessary rather than sufficient condition is made clear by examination of Eq. (16): vanishing of the left-hand side only implies that the number of mechanisms and states of self-stress are equal, not that each equals zero.

Maxwell's criterion gives insight into the design of lattice materials, and reveals why foams are almost always bending-dominated [23–25]. Examples of some idealized cell shapes are shown in Fig. 10. Isolated cells that satisfy Maxwell's criterion and are rigid are labeled "YES", while "NO" means the Maxwell condition is not satisfied and that the cell is a mechanism. It is generally assumed that the best model for a cell in a foam approximates a space-filling shape. However, none of the space-filling shapes (indicated by numbers 2, 3, 4, 6, and 8) are rigid. In fact no single space-filling polyhedral cell has $M \geq 0$. Space-filling combinations of cell shapes, by contrast, exist that have $M \geq 0$; for example, the tetrahedron and octahedron in combination fill space to form a rigid framework.

Maxwell's criterion gives a prescription for designing stretch-dominated lattices, which we now examine.

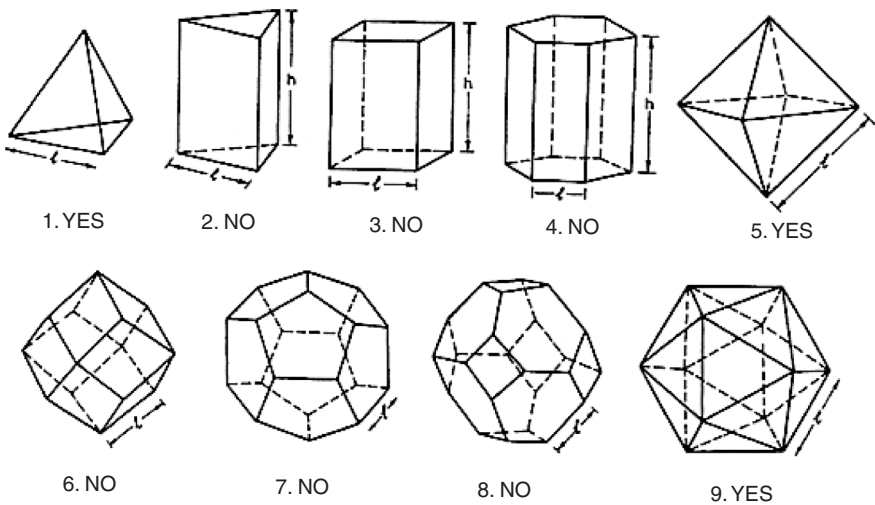


Fig. 10 Polyhedral cells. Those that are space filling (2–4, 6, 8) all have $M < 0$, that is, they are bending-dominated structures.

1.1.5

Stretch-Dominated Structures

Figure 11 shows an example of a microtruss lattice structure. For this structure $M = 18$; it has no mechanism and many possible states of self-stress. It is one of many structures for which $M \geq 0$, and its mechanical response is stretch-dominated. In this section we review briefly the properties of stretch-dominated microtruss lattice materials, using the same approach as that of Section 1.1.3.

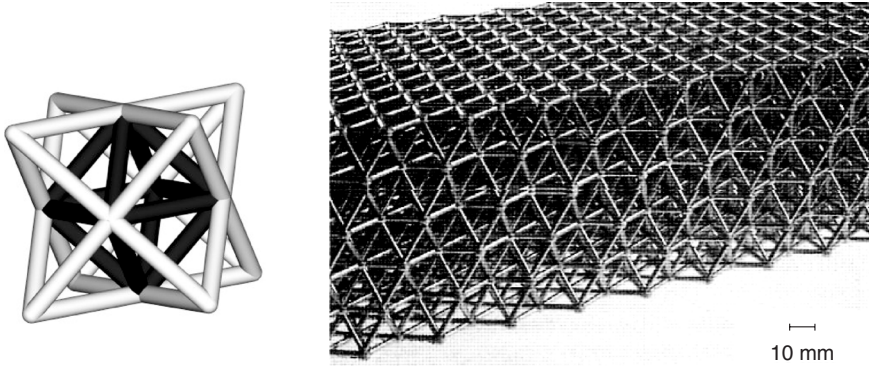


Fig. 11 A microtruss structure with $M > 0$, together with its unit cell.

Consider the tensile loading of the material. Since it has no mechanisms, the structure first responds by elastic stretching of the struts. On average one-third of its struts carry tension when the structure is loaded in simple tension, regardless of the loading direction. Thus

$$\frac{\tilde{E}}{E_s} \approx \frac{1}{3} \left(\frac{\tilde{\rho}}{\rho_s} \right) \quad (\text{stretch-dominated behavior}). \quad (19)$$

The elastic limit is reached when one or more sets of struts yields plastically, buckles, or fractures; the mechanism with the lowest collapse load determines the strength of the structure as a whole. If the struts are plastic, the collapse stress – by the same argument as before – is

$$\frac{\tilde{\sigma}_{pl}}{\sigma_{y,s}} \approx \frac{1}{3} \left(\frac{\tilde{\rho}}{\rho_s} \right) \quad (\text{plastic stretch-dominated behavior}). \quad (20)$$

This is an upper bound since it assumes that the struts yield in tension or compression when the structure is loaded. If the struts are slender, they may buckle before they yield. Then, following the same reasoning that led to Eq. (7), the “buckling strength” scales as

$$\frac{\tilde{\sigma}_{el}}{E_s} \propto \left(\frac{\tilde{\rho}}{\rho_s} \right)^2 \quad (\text{buckling-dominated behavior}). \quad (21)$$

The only difference is the magnitude of the constant of proportionality, which depends on the details of the connectivity of the strut. But remembering that buckling of a strut depends most importantly on its slenderness t/L , and that this is directly related to relative density, we do not expect the dependence on configuration to be strong. In practice elastomeric foams always fail by buckling; rigid polymer and metallic foams buckle before they yield when $\tilde{\rho}/\rho_s \leq 0.05$ and $\tilde{\rho}/\rho_s \leq 0.01$, respectively.

Failure can also occur by strut fracture. A lattice structure made from a ceramic or other brittle solid will collapse when the struts start to break. Stretch domination means that the struts carrying tension will fail first. Following the argument that led to Eq. (18) we anticipate a collapse stress $\tilde{\sigma}_{cr}$ that scales as

$$\frac{\tilde{\sigma}_{cr}}{\sigma_{cr,s}} \propto \left(\frac{\tilde{\rho}}{\rho_s} \right) \text{ (stretch-fracture-dominated behavior)} \quad (22)$$

where $\sigma_{cr,s}$ is now the tensile fracture strength of the material of a strut. Here the constant of proportionality is less certain. Brittle fracture is a stochastic process, dependent on the presence and distribution of defects in the struts. Depending on the width of this distribution, the failure of the first strut may or may not trigger the failure of the whole.

The main thing to be learnt from these results is that both the modulus and initial collapse strength of a stretching-dominated lattice are much greater than those of a bending-dominated cellular material of the same relative density. This makes stretch-dominated cellular solids the best choice for lightweight structural applications. But because the mechanisms of deformation now involve “hard” modes (tension, compression) rather than “soft” ones (bending), initial yield is followed by plastic buckling or brittle collapse of the struts, which leads to post-yield softening (Fig. 12). This makes them less good for energy-absorbing applications, which require a stress–strain curve with a long, flat plateau. This post-yield regime ends and the stress rises steeply at the densification strain, given, as before, by Eq. (9).

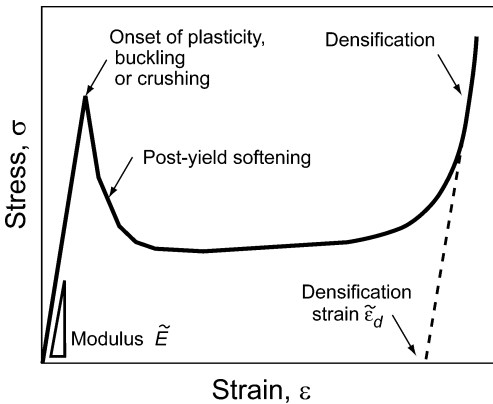


Fig. 12 Schematic stress–strain curve for a stretch-dominated structure. It has high stiffness and high initial strength, but can show post-yield softening.

These results are summarized in Figs. 13 and 14, in which the relative modulus \tilde{E}/E_s and strength $\tilde{\sigma}/\sigma_s$ are plotted against relative density $\tilde{\rho}/\rho_s$. They show the envelopes within which the currently-researched cellular structures lie. In Fig. 13, the two broken lines show the locus of relative stiffness as the relative density changes for ideal stretch- and bending-dominated lattices made of the material lying at the point (1,1). Stretch-dominated, prismatic microstructures have moduli that scale as $\tilde{\rho}/\rho_s$ (slope 1); bending-dominated, cellular microstructures have moduli that scale as $(\tilde{\rho}/\rho_s)^2$ (slope 2). *Honeycombs*, a prime choice as cores for sandwich panels and as supports for exhaust catalysts, are extraordinarily efficient; if loaded precisely paral-

parallel to the axis of the hexagons, they lie on the “ideal-stretch” line. In directions normal to this they are exceptionally compliant. *Foams*, available in a wide range of densities, epitomize bending-dominated behavior. If ideal, their relative moduli would lie along the lower broken line. Many do, but some fall below. This is because of the way they are made [4]; their structure is often heterogeneous, strong in some places, weak in others; the weak regions drag down both stiffness and strength. *Woven structures* are lattices made by three-dimensional weaving of wires; at present these are synthesized by brazing stacks of two-dimensional wire meshes, giving configurations that are relatively dense and have essentially ideal bending-dominated properties. There is potential for efficient low-density lattices here; it requires the ability to weave three-dimensional meshes. *Pyramidal lattices* have struts configured as if along the edges and base of a pyramid – Fig. 11 is an example. They are fully triangulated and show stretch-dominated properties but lie by a factor of 3 below the ideal line. *Kagome lattices* – the name derives from that of Japanese weaves – are more efficient; they offer the lowest mass-to-stiffness ratio.

Strength (Fig. 14) has much in common with stiffness, but there are some differences. The “ideals” are again shown as broken lines. Stretch-dominated, prismatic microstructures have strengths that scale as $\tilde{\rho}/\rho_s$ (slope 1); bending dominated scale as $(\tilde{\rho}/\rho_s)^{3/2}$ (slope 1.5). Honeycombs, even when compressed parallel to the hexagon

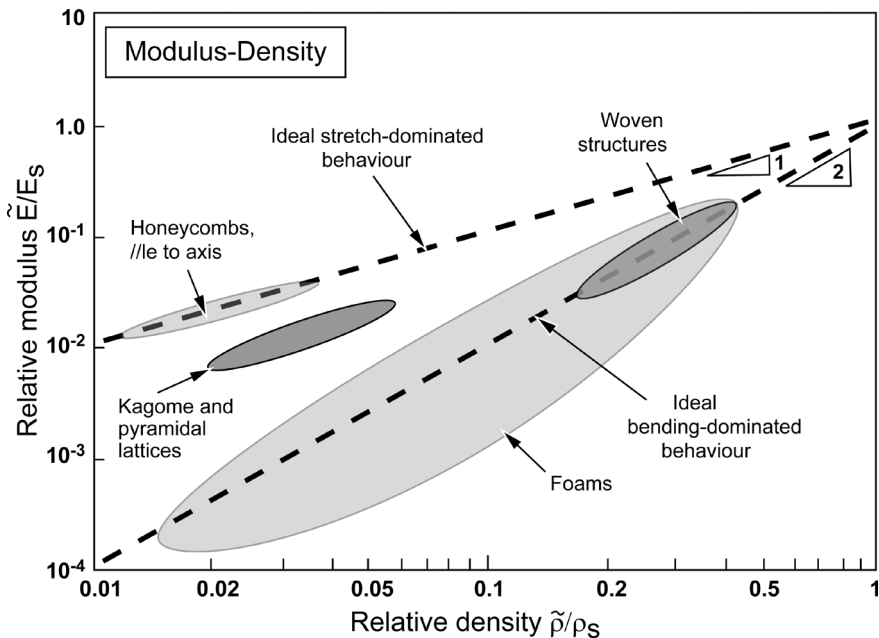


Fig. 13 Relative modulus against relative density on logarithmic scales for cellular structures with different topologies. Bending-dominated structures lie along a trajectory of slope 2, and stretch-dominated structures along a line of slope 1.

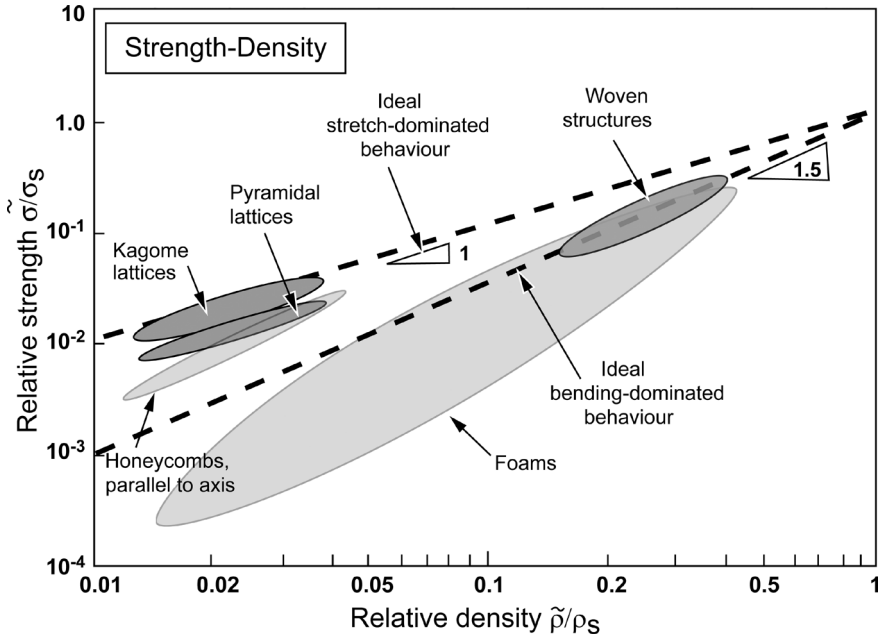


Fig. 14 Relative strength against relative density on logarithmic scales for cellular structures with different topologies. Bending-dominated structures lie along a trajectory of slope 1.5, and stretch-dominated structures along a line of slope 1.

axis, fall below the ideal because the thin cell walls buckle easily. Metallic foams, similarly underperform – none reach the ideal bending-dominated performance line, a consequence of their imperfections. The current generation of woven structures lies on the bending-dominated ideal. As with stiffness, pyramidal and Kagome lattices offer near-ideal stretch-dominated performance.

The bending/stretching distinction influences mechanical properties profoundly, but has no effect on *thermal* or *electrical properties*. At the approximate level we seek in this overview, they are adequately described by Eqs. (11)–(13).

1.1.6

Summary

Structural engineers have known and used latticelike structures for generations, but it is only in the last 20 years that an understanding of *materials* with a lattice-like structure has emerged. Many of these respond to stress in precisely the way engineers seek to avoid – by bending deformation of the struts that make up the structure. As materials, these are interesting for their low stiffness and strength, and the large strains they can accommodate – properties that are attractive in cushioning, packaging, and energy absorption and in accommodating thermal shock. But if stiff-

ness and strength at low weight are sought, the lattice must be configured in such a way that bending is prevented, leaving strut-stretching as the dominant mode of deformation. This suggests the possibility of a family of microtruss structured materials, many as yet unexplored.

With this introduction, we are ready to explore the design and characterisation of ceramic cellular materials in more detail in the chapters that follow.

Acknowledgements

Many people have contributed to the ideas reported in this chapter. I particularly wish to recognize the contributions of Profs. L.J. Gibson, N.A. Fleck, A.G. Evans, J.W. Hutchinson, and H.N.G. Wadley, the fruits of long collaborations.

References

- 1 Gent, A.N., Thomas, A.G. *J. Appl. Polym. Sci.* **1959**, 1, 107.
- 2 Patel, M.R., Finnie, I. *J. Mater.* **1970**, 5, 909
- 3 Gibson, L.J., Ashby, M.F. *Cellular Solids, Structure and Properties*, 2nd ed., Cambridge University Press, Cambridge, UK, 1997.
- 4 Ashby, M.F., Evans, A.G., Fleck, N.A., Gibson, L.J., Hutchinson, J.W., Wadley, H.N.G. *Metal Foams: A Design Guide*, Butterworth Heinemann, Oxford, UK., 2000.
- 5 Banhart, J. (Ed.) *Metallschäume*, MIT Verlag, Bremen, Germany, 1997.
- 6 Banhart, J., Ashby, M.F., Fleck, N.A. (Eds.) *Metal Foams and Foam Metal Structures*, Proc. Int. Conf. Metfoam '99, MIT Verlag, Bremen, Germany, 1999.
- 7 Banhart, J., Ashby, M.F., Fleck, N.A. (Eds.) *Metal Foams and Foam Metal Structures*, Proc. Int. Conf. Metfoam '01, MIT Verlag, Bremen, Germany, 2001.
- 8 Banhart J., Fleck, N.A. (Eds), *Metal Foams and Foam Metal Structures*, Proc. Int. Conf. Metfoam '03, MIT Verlag, Bremen, Germany, 2003.
- 9 Schwartz, D.S., Shih, D.S., Evans, A.G., Wadley, H.N.G. (Eds.) *Porous and Cellular Materials for Structural Applications*, Materials Research Society Proceedings Vol. 521, MRS, Warrendale, PA, USA, 1998.
- 10 Brezny, R., Green, D.J. *J. Am. Ceram. Soc.* **1989**, 72, 1145–1152.
- 11 Brezny, R., Green, D.J. *Acta Metall. Mater.* **1990**, 38, 2517–2526.
- 12 Brezny, R., Green, D.J. *J. Am. Ceram. Soc.* **1991**, 74, 1061–1065.
- 13 Nanjangud. S.C., Brezny, R., Green, D.J. *J. Am. Ceram. Soc.* **1995**, 78, 266–268.
- 14 Huang, J.S., Gibson, L.J. *Acta Metall. Mater.* **1991**, 39, 1617–1626.
- 15 Huang, J.S., Gibson, L.J. *Acta Metall. Mater.* **1991**, 39, 1627–1636.
- 16 Huang, J.S., Gibson, L.J. *J. Mater. Sci. Lett.* **1993**, 12, 602–604.
- 17 Triantafyllou, T.C., Gibson, L.J. *Int. J. Mech. Sci.* **1990**, 32, 479–496.
- 18 Vedula, V.R., Green, D.J., Hellman, J.R. *J. Eur. Ceram. Soc.* **1998**, 18, 2073–2080.
- 19 Vedula, V.R., Green, D.J., Hellman, J.R., Segall, A.E. *J. Mater. Sci.* **1998**, 33, 5427–5432.
- 20 Maxwell, J.C. *Philos. Mag.* **1864**, 27, 294.
- 21 Calladine, C.R. *Theory of Shell Structures*, Cambridge University Press, Cambridge, UK, 1983.
- 22 Pellegrino, S., Calladine, C.R. *Int. J. Solids Struct.* **1986**, 22(4), 409.
- 23 Deshpande, V.S., Ashby, M.F., Fleck, N.A. *Acta Metall. Mater.* **2001**, 49, 1035–1040.
- 24 Deshpande, V.S., Fleck, N.A., Ashby, M.F. *J. Mech. Phys. Solids* **2001**.
- 25 Guest, S.D. *Philos. Trans. R. Soc. Lond. A*, **2000**, 358, 229–243.